Neural Processing Letters
https://doi.org/10.1007/s11063-019-10008-w

Surface Electromyography-Based Daily Activity Recognition Using Wavelet Coherence Coefficient and Support Vector Machine

Xugang Xi[1] · Chen Yang[1] · Jiahao Shi[1] · Zhizeng Luo[1] · Yun-Bo Zhao[2]

Abstract
Daily activity monitoring plays an important role among frail or elderly people and has caught attention. Surface electromyography (sEMG) can extract the feature of activity, but it is not stable because of electrode displacement, postural changes, and individual-dependent features, such as the condition of muscles, subcutaneous fat, and skin surface. To effectively extract the feature of sEMG signal, we proposed a new method of feature extraction based on coherence analysis. The sEMG signals were recorded from gastrocnemius, tibialis anterior, rectus femoris, and semitendinosus. After de-noising, sEMG signals were decomposed into 32-scale by wavelet transformation, and their wavelet coefficients were employed to calculate wavelet coherence coefficients (WCC). We employed *T* test to find out if the coherence between sEMG signals was statistically different among six activities. The 32nd scale WCC of RF–ST and ST–TA as eigenvector was entered into the support vector machine (SVM). The six activities, namely, standing, walking, running, stair-ascending, stair-descending, and falling, were successfully identified by the WCC feature with the SVM classifier.

Keywords Electromyography · Activity recognition · Wavelet transforms · Wavelet coherence coefficients · Support vector machine

1 Introduction

In the past decade, the aging population showed a steady growth. Elders are living alone, and helping them live better is social responsibility. Activity recognition has caught attention, which is fundamental for activity monitoring and fall detection [1]. The methods of monitoring activities can be divided into three categories: computer

✉ Xugang Xi
xixi@hdu.edu.cn

✉ Zhizeng Luo
luo@hdu.edu.cn

[1] School of Automation, Hangzhou Dianzi University, Hangzhou 310018, China

[2] College of Information Engineering, Zhejiang University of Technology, Hangzhou 310023, China

Published online: 26 February 2019

vision, ambient, and wearable sensor [2]. Computer vision-based method requires equipment with multiple-view cameras that must be used indoors [3–5]. The frequency of vibrations generated by daily living activities (ADLs) is processed to detect activity in the ambient sensor-based method. The sensors for monitoring include infrared sensors, door contacts, radars, and microphones [6]. This method can effectively obtain information on human daily activities but suffers from disadvantages of fixed application scenario and cumbersome installation. Compared with visual or ambient sensors, wearable sensors exhibit advantages including convenient operation, physical environments compatibility and outdoor feasibility [7, 8]. Wearable sensors include kinematic or electrophysiological sensors. The sensors must be worn in the human body. Wireless and wearable sensors, such as accelerator sensors, inertial sensors, gyroscopes [9], and surface electromyography (sEMG) sensors, have been widely used in activity awareness [10].

sEMG sensors are widely applied in activity recognition, gait analysis, and prosthetic control [11]. Compared with other wearable sensors, sEMG sensors can directly indicate the electrophysiological responses of the human body to various activities. sEMG offers the inherent advantages of predicting movements, distinguishing passive and active activities, and achieving a short calculation time. Triloka et al. [12] presented a sEMG based walking gait identification by multilayer feed-forward neural network, achieving accuracy of 98%. Young et al. [13] classified walking, ramps, and stairs using sEMG in eight amputee subjects, results that reduced the average transitional error from 18.4 to 12.2% and the average steady-state error from 3.8 to 1.0%. Cheng et al. [14] presented a framework for activity monitoring by sEMG and accelerometer signals, and obtained a recognition accuracy of $>98\%$. However, considerable challenges continue to exist in searching for the best feature set from original sEMG datasets [15]. The sEMG can be influenced by many disturbing factors, such as electrode displacement, postural changes, and individual-dependent features, such as condition of muscles, subcutaneous fat, and skin surface [16]. sEMG is sensitive to external factors, such as experimental setting, recording site, or natural environment.

Wavelet transformation is widely used in sEMG processing [17]. It decomposes sEMG into many sub-bands including accurate information [15]. Coherence analyzes the relation between two signals in time–frequency space, which is popular and useful in digital signal analysis, especially in wavelet transformation [18]. For example, Lou et al. [19] implemented Fourier transform coherence and cortico-muscular coherence (CMC) analysis to recognize finger extension, finger flexion, thumb adduction, and rest. The best accuracies across subjects are at 81.00 7.34%. However, sEMG recording is a non-stationary recording, which means that the spectrum changes over time. Therefore, coherence must be regarded as a dynamic quantity, and wavelet transformation is the most suitable for monitoring spectral density development [20]. For instance, Imoto et al. [21] studied the mechanism of coordinated movement between agonist muscle and antagonist muscle using wavelet coherence analysis of sEMG. They concluded that a stable condition tended to show higher correlation than instability condition. Usually, wavelet coherence can be used to analyze non-stationary random signals, such as sEMG and electroencephalograms (EEG). However, EEG is vulnerable to external factors, such as eye signals and visual feedback, which interfere with signal collection process. The drive that leads to CMC can also cause muscular coherence between co-activated active muscle groups in the same activities. sEMG coherence may provide a cortical muscle-coupling message [22]. However, ADL recognition based on sEMG coherence analysis is less studied, inspiring many researchers to fill the gap.

The classification technique is another important issue for activity monitoring. Support vector machine (SVM) and neural networks have been widely applied to classify human movement based on sEMG [23]. SVM analyze data used for classification, which constructs a hyperplane or set of hyperplanes in a high- or infinite-dimensional space to separate different datasets [24]. Compared with neural network, SVM generate a relatively straightforward solution for an optimization problem. SVM is suitable for a classification system based on sEMG with high-dimensional feature vectors. For example, Chen et al. [25] employed a multikernel learning SVM to recognize multiple finger movements and obtained the highest recognition accuracy of 97.93%.

In this paper, we propose a novel sEMG feature extraction method based on wavelet coherence coefficient (WCC) for daily activity recognition. WCC of sEMG is incorporated into support vector machine to classify daily activity, which shows a relatively high degree of accuracy. Section II introduces activity definition, data acquisition, and proposed feature extraction and classification method. Section III analyzes and discusses experiments and results. Section IV presents conclusions.

2 Materials and Method

First, we will provide a description of the experimental procedure and sEMG preprocess. A new feature extraction method is then introduced based on wavelet coherence analysis. The wavelet coherence analysis and difference analysis are used to select features. Finally, the feature vectors are entered into three classifiers, SVM, fuzzy min–max neural networks (FMMNN), and multi-layer perceptron (MLP) neural network. The block diagram of the proposed sEMG-based daily activity recognition method is presented in Fig. 1.

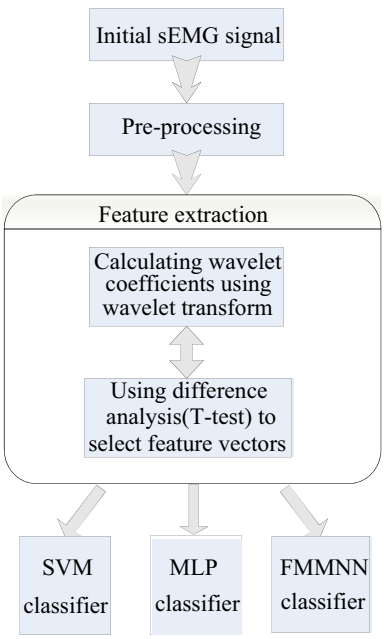

Fig. 1 sEMG-based daily activity recognition

2.1 Activities of Daily Life and Muscles

Recognizing normal activity and distinguishing falls from daily activities are two important issues to accomplish daily activity monitoring and fall detection. The most common six ADLs, namely, standing, running, walking, stair-ascending, and stair-descending, were selected. These activities result from contraction of lower limb muscles. Thus, we recorded sEMG signals from gastrocnemius (GA), tibialis anterior (TA), rectus femoris (RF), and semitendinosus (ST) in the left lower limb, marked by CH1 through CH4, as showed in Fig. 2. The gastrocnemius is primarily involved in running, jumping and other "fast" movements of leg, and to a lesser degree in walking and standing. The tibialis anterior is responsible for dorsiflexing and inverting the foot. The rectus femoris is the flexors of the thigh at the hip. The semitendinosus work to flex the knee and extend the hip.

2.2 Activities Experimental Procedure

We collected data from five healthy subjects, three of which are males and two are females, with a mean age 24.13 ± 1.36 years old. We did not choose old and disabled individuals in the experiment since they may not be suitable to conduct long-time and substantial movements, and the relative trend of each feature extraction and pattern recognition algorithm would remain the same for both young and old, resulting in no considerable difference in inherent characteristics of EMG signals between subjects with and without disabilities [26, 27]. The experimental activities include standing, walking, running, stair-ascending, stair-descending, and falling (Fig. 3). The subjects execute six activities in order for 20 s each in a session, with 5 s rest between each activity. They performed over 60 sessions each, separated by 30 s rest period.

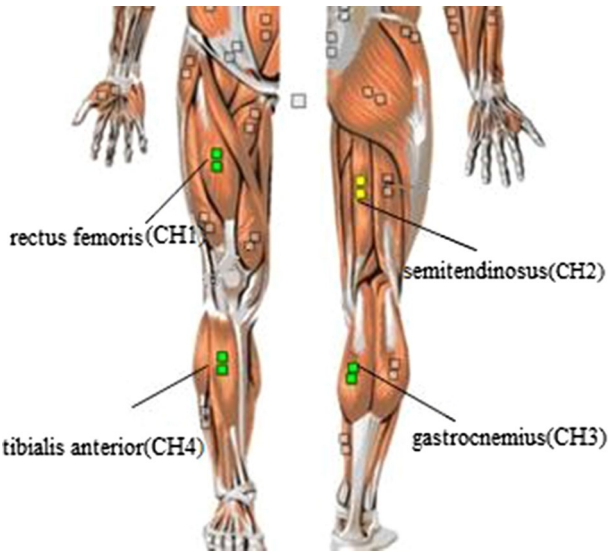

Fig. 2 Description of muscle location and sEMG electrode placement. Gastrocnemius (GA), tibialis anterior (TA), rectus femoris (RF), and semitemdinosus (ST)

Fig. 3 Activities experimental procedure, **a** standing, **b** walking, **c** running, **d** stair-ascending, **e** stair-descending, **f** falling

2.3 Data Acquisition and Preprocessing

We recorded the sEMG at 1024 Hz sampling frequency using Trigno™ Wireless EMG (Delsys Inc., Natick, MA, USA) with 20–450 Hz bandwidth, 16-bit resolution (12 dB/octroll-off), and a baseline noise of < 1.25 uV (rms) (Fig. 4). All data processing and analysis were performed in MATLAB with customized programs. The recorded signals are pre-processed using Empirical Mode Decomposition to remove unwanted noise [28]. Figure 5 shows the signal after de-noising.

2.4 Wavelet Transformation

A wavelet is a mathematical tool used to divide a signal into different scale components. Compared with Fourier transform, wavelets are localized in both time and frequency. A signal can be decomposed by Wavelet analysis via a basis functions. The convolution of the signal $x(t)$ with the scaled mother wavelet function $\varphi(t)$ produces Wavelet coefficients $W_x(a, b)$.

$$W_x(a,b) = \langle x, \varphi_{a,b} \rangle = \frac{1}{\sqrt{a}} \int_{-\infty}^{\infty} x(t) \varphi^* \left(\frac{t-b}{a} \right) dt \tag{1}$$

Fig. 4 Activities experimental procedure

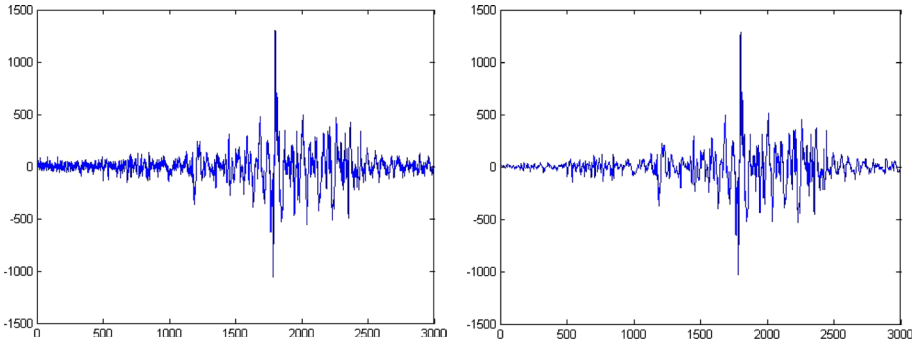

Fig. 5 The semitemdinosus sEMG signal of falling, **a** before noise reduction, **b** after noise reduction

where a is the scale of the wavelet, and t is the local time origin of the analyzing wavelet.

In this paper, an improved Morlet mother wavelet function $\varphi(\omega)$ was used.

$$\varphi(\omega) = \sigma\left[\exp\left(\frac{-(\omega-p)^2\sigma^2}{2}\right) - \exp\left(\frac{-(\omega-p)^2\sigma^2}{4}\right)\exp\frac{-p^2\sigma^2}{4}\right] \tag{2}$$

where σ is the parameter that controls Morlet wavelet decay, p is the parameter of frequency, usually $p > 5$. A variation in σ enables changing the adaptive window width.

2.5 Wavalet Coherence Coefficient

We employed wavelet coherence coefficient (WCC) to evaluate sEMG cross-correlation in time and frequency. The cross-wavelet power of two signals $x(t)$ and $y(t)$ is defined as [29]:

$$W_{xy}(a,b) = W_x(a,b)W_y^*(a,b) \tag{3}$$

The cross-wavelet power represents the local covariance between two signals at each scale. Because the wavelet coherence is a measure of local correlation in time and scale of sEMG, it is considered as a very useful tool to detect activity based sEMG. The wavelet coherence coefficients (WCC) is defined as [30]:

$$R_{xy}(a,b) = \frac{\left|S(W_{xy}(a,b))\right|}{\left[S\left(\left|W_x(a,b)\right|^2\right)S\left(\left|W_y(a,b)\right|^2\right)\right]^{\frac{1}{2}}} \tag{4}$$

The value of WCC is in the range of $0 \le R_{xy}(a,b) \le 1$. The value close to 1 indicates high correlation, whereas that close to 0 represents weak correlation. Based on the mentioned theory, wavelet coherence is a suitable method to study the signal over time [31, 32]. We employed wavelet coherence to investigate the sEMG signals.

Furthermore, the observations are drawn from a normally distributed data set and the different sets have the same variance, satisfying the essential assumption of T test. So that T test is applied to check whether the coherence value at six types of muscle combinations significantly differ across activities. Independent sample T test is defined as:

$$t = \frac{\bar{X}_1 - \bar{X}_2}{\sqrt{\frac{(n_1-1)S_1^2+(n_2-1)S_2^2}{n_1+n_2-2}\left(\frac{1}{n_1}+\frac{1}{n_2}\right)}} \tag{5}$$

where S_1^2 and S_2^2 are sample variance. n is sample size.The confidence coefficient is defined as:

$$C_\psi = 1 - (1-\psi)^{\frac{1}{N-1}} \tag{6}$$

where N is the number of samples, ψ is confidence level. In our study, ψ is 95%, which correspond to a P value of 0.05. C_ψ represents the confidence limit. If the value is above C_ψ, we consider that the coherence is significant.

2.6 Classification Method

(1) Support Vector Machine (SVM)

SVM analyze data used for classification, which constructs a hyperplane or set of hyperplanes in a high- or infinite-dimensional space to separate different datasets [23].

SVM requires computing the following optimization problem amounts to minimizing an expression of the form:

$$0.5\left\|\omega^2\right\| + \frac{1}{N}\sum_{i=1}^{N}\xi_i \tag{7}$$

subject to:

$$y_i\left[(x_i \cdot \omega) + b\right] \geq 1 - \xi_i, \quad i - 1,\ 2,\ \ldots,\ N \tag{8}$$

where x_i is an p-dimensional real vector (p is 2 in this study, and represents two independent inputs), y_i are either 1 or -1, b is a offset, N is the number of samples, ω is the normal vector to the hyperplane, ξ_i is the smallest nonnegative number satisfying Eq. (8).

To be computed easily, Eq. (9) is defined in terms of a kernel function.

$$f(x) = \mathrm{sgn}\left(\sum_{i=1}^{N} a_i y_i k(x,\ x_i) + b\right) \tag{9}$$

where $k(x, x_i)$ is a kernel function, the coefficients a_i are obtained by solving the optimization problem. In this paper, we used Radial Basis Function as the kernel function. The hyperparameters C is 0.9 and gamma is 0.35.

2. Fuzzy Min–Max Neural Networks (FMMNN)

The FMMNN is based on the hyperbox fuzzy sets [33]. A hyperbox is defined by its minimum and maximum points which are created by the input patterns. The membership function is set with respect to the minimum and maximum points of the hyperbox. Its multilayer structure is capable of dealing with a nonlinear separability issue. It also possesses an adaptive learning capability.

3. Multi-Layer Perceptron (MLP)

MLP is an artificial neural network with collection of units, neurons or nodes, which are simple processors whose computing ability is restricted to a rule for combining input to calculate an output signal [34]. Output signals may be sent to other units along connections known as weights.

3 Results

3.1 Classification Method Results of Feature Selection

We calculated the WCC of six kinds of muscle combinations (i.e., RF–ST, ST–TA, RF–TA, RF–GA, ST–GA, and GA–TA) after 32-scale wavelet decomposition of sEMG signals. The averages of WCC on different scales in six activities are shown in Fig. 6. The WCC is maximal at the 32nd scale. Therefore, the 32th scale WCC is selected. Figure 7 presents a histogram of the 32th scale WCC between different muscles in six ADLs. The

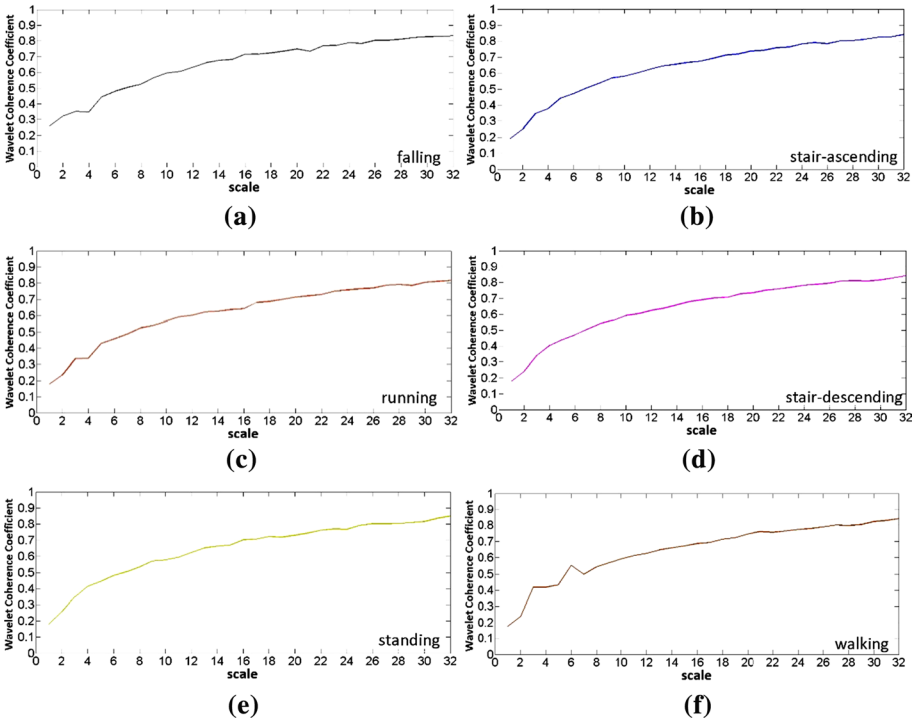

Fig. 6 The average WCC of six kinds of muscle combinations on different scales in six activities, **a** is falling, **b** is stair-ascending, **c** is running, **d** is stair-descending, **e** is standing, **f** is walking

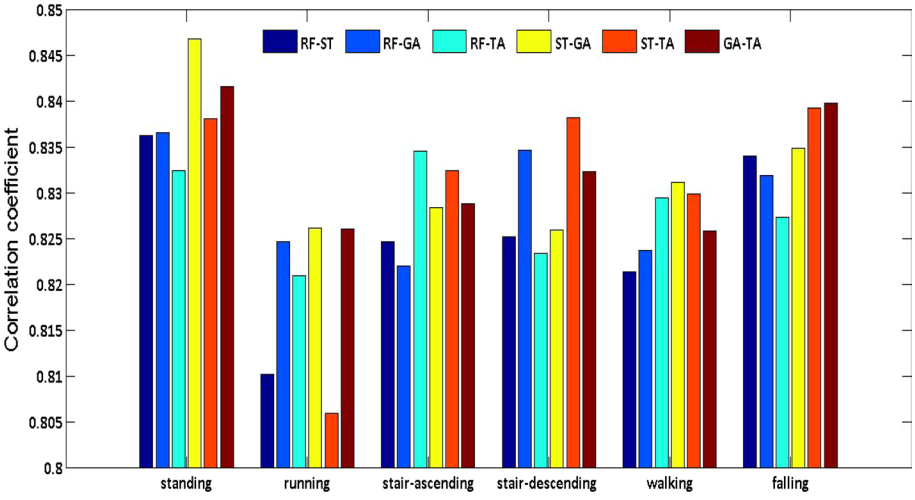

Fig. 7 The histogram of WCC between different muscles in 6 ADL

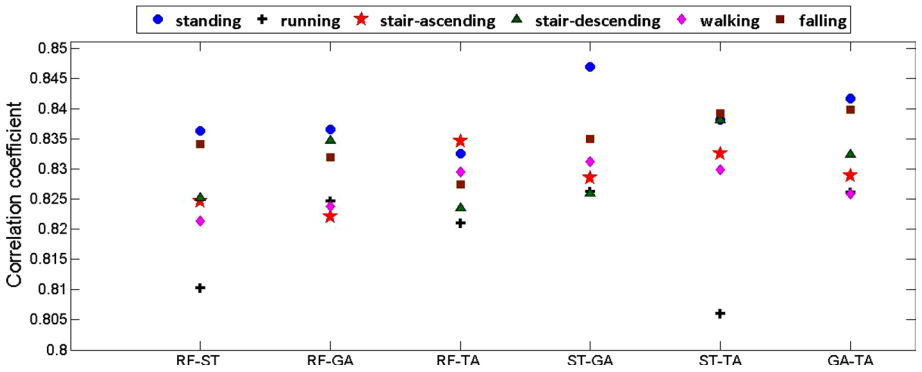

Fig. 8 Scatter diagrams of WCC between different muscles in six ADLs

WCC is between 0.8 and 0.85. The WCC of standing and running is the highest and lowest, respectively.

Figure 8 presents scatter diagrams of the 32th scale WCC between different muscles in six ADLs. Figure 8 shows that the separability of RF–ST and ST–TA are better than that of RF–TA, RF–GA, ST–GA, and GA–TA.

Furthermore, *T* test was applied to check for significant differences. Statistical tests were performed using SPSS. The difference analysis of WCC between two different ADLs is shown in Table 1. Sig. represents significant difference, a value of which that is below 0.05 represents a significant difference. All sig. of RF–ST between two activities are 0, except the combination between stair-ascending and stair-descending. All sig. of ST–TA are 0 or 0.001, except two kinds of combination. It shows that RF–ST and ST–TA have

Table 1 The sig. of muscle combination between two different ADLs

Activities	Muscle combination					
	RF–ST	RF–GA	RF–TA	ST–GA	ST–TA	GA–TA
Stair-ascending and stair-descending	0.809	0.000	0.000	0.211	0.001	0.040
Stair-ascending and running	0.000	0.085	0.000	0.179	0.000	0.179
Stair-ascending and standing	0.000	0.000	0.274	0.179	0.001	0.000
Stair-ascending and walking	0.000	0.000	0.561	0.000	0.901	0.063
Stair-ascending and falling	0.000	0.000	0.000	0.000	0.000	0.000
Stair-descending and running	0.000	0.000	0.177	0.974	0.000	0.000
Stair-descending and standing	0.000	0.353	0.000	0.974	0.976	0.000
Stair-descending and walking	0.000	0.016	0.000	0.000	0.001	0.842
Stair-descending and falling	0.000	0.006	0.000	0.000	0.000	0.000
Running and standing	0.000	0.000	0.000	0.000	0.000	0.000
Running and walking	0.000	0.000	0.000	0.000	0.000	0.002
Running and falling	0.000	0.000	0.000	0.000	0.000	0.000
Standing and walking	0.000	0.159	0.705	0.000	0.001	0.000
Standing and falling	0.000	0.059	0.000	0.000	0.000	0.000
Walking and falling	0.000	0.625	0.000	0.000	0.000	0.000

more activities with sig. below 0.05, meaning that the significant difference of RF–ST and ST–TA are better than other muscle combinations.

According to the separability and difference analysis, the WCC of RF–ST and ST–TA was selected as the feature.

3.2 Result of Classification

The WCC of RF–ST and ST–TA was entered to the SVM to classify falling, standing, walking, running, stair-ascending, and stair-descending. The classification results by SVM are compared with FMMNN and MLP. The classification performance was evaluated by the sensitivity (SEN), specificity (SPE), accuracy (ACC), and the area under the receiver operating characteristic curve (ROC-AUC) [35].

$$SEN = \frac{TP}{TP + FN} \tag{10}$$

$$SPE = \frac{TN}{TN + FP} \tag{11}$$

$$ACC = \frac{(TP + TN)}{TP + FP + FN + TN} \tag{12}$$

True positive (TP) a target activity occurs, and the classifier detects it.

False positive (FP) the classifier announces a target activity, but it does not occur.

True negative (TN) a non-target activity is performed, but the classifier does not declare a target activity.

False negative (FN) a target activity occurs, but the classifier does not detect it.

A receiver operating characteristic (ROC) curve indicates the trade-off between the sensitivity and specificity of a classifier [36], allowing us to examine how the *FP* and *TP* rates change as the threshold used to determine a match is altered. A useful score for integrating these two characteristics is the ROC-AUC score [37].

We used a fourfold cross validation. The result of average sensitivity and specificity over four sub-data sets are shown in Fig. 9 and Table 2.

The SVM classifier exhibits great performance for all activities. The average sensitivity of SVM is 95.98%, the average specificity of SVM is 94.20%, the average accuracy of SVM is 95.17%, and the average ROC-AUC is 0.95. The sensitivity, specificity, and accuracy of standing and falling are 100%, which indirectly reflects the WCC with SVM is suitable to recognize standing and falling. Figure 7 also shows that the WCC of falling and standing is higher than other activities, indicating that activities with high WCC can be easily recognized. Running features relatively low specificity, sensitivity, accuracy, and ROC-AUC. The reason may be that abnormal co-active muscle, electrode vibration, or sweat in sharp running causes unstable sEMG [38, 39]. Furthermore, FMMNN and MLP demonstrate weak performance. The average accuracy drops to 90.89% and 92.04%, the average ROC-AUC drops to 0.91 and 0.92, respectively. The SVM is superior to FMMNN and MLP in terms of activity recognition.

The WCC was compared with six features, within which the average sensitivity, specificity, accuracy and ROC-AUC for seven features with three classifiers are shown in Table 3. The sensitivity of WCC is higher than the six other features. Although the specificity of the other features is higher than that of WCC, the sensitivity is below 83.33%,

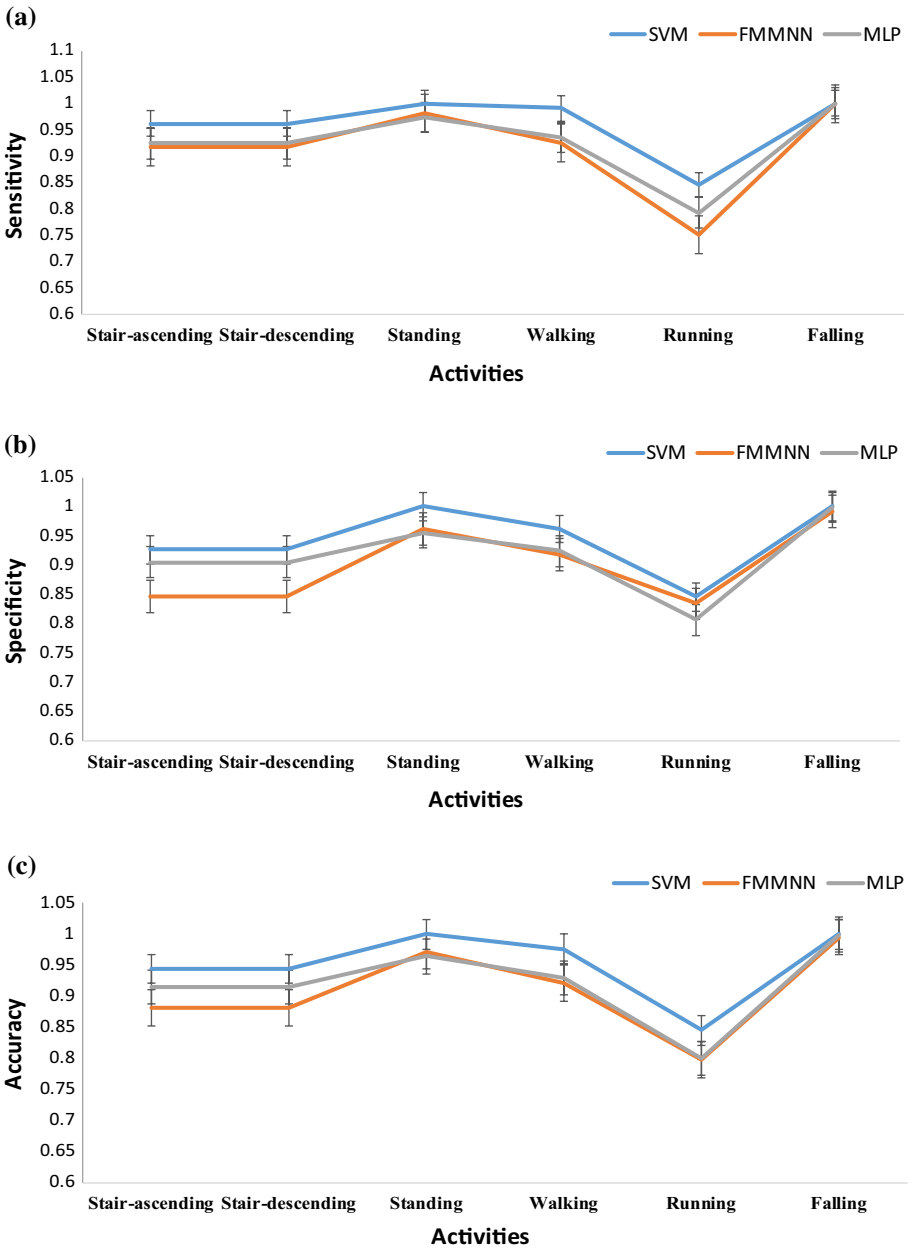

Fig. 9 Average sensitivity, specificity, and accuracy of seven ADLs by SVM, FMMNN, and MLP. **a** Average sensitivity (error bar: standard error), **b** average specificity (error bar: standard error), **c** average accuracy (error bar: standard error)

Table 2 The average sensitivity, specificity, accuracy and ROC-AUC of seven ADLs by SVM, FMMNN, and MLP (SEN %, SPE %, ACC %, ROC-AUC)

	SVM				FMMNN				MLP			
Stair-ascending	96.15	92.56	94.43	0.93	91.66	84.52	88.23	0.89	92.35	90.46	91.45	0.91
Stair-descending	96.15	92.56	94.43	0.93	91.66	84.52	88.23	0.89	92.35	90.46	91.45	0.91
Standing	100	100	100	1	98.07	96.15	97.24	0.96	97.32	95.45	96.43	0.96
Walking	99.04	96.15	97.63	0.97	92.56	91.66	92.18	0.92	93.48	92.39	92.97	0.93
Running	84.52	84.52	84.52	0.84	75.15	83.33	79.86	0.81	79.24	80.56	79.98	0.80
Falling	100	100	100	1	100	99.04	99.56	0.99	100	99.86	99.94	0.99
Average	95.98	94.20	95.17	0.95	93.18	89.87	90.89	0.91	92.45	91.53	92.04	0.92

which is too low for activity recognition. The sensitivity, specificity, accuracy and ROC-AUC of SVM for all features is higher than those of FMMNN and MLP. Therefore, the WCC with SVM exhibits the best performance in our paper.

4 Conclusion

Daily activity monitoring and fall detection is very important for the people who need assistance in their daily life, such as the elderly or frail. In this paper, we focus on ADL monitoring, which is mainly involved in standing, walking, running, stair-ascending, stair-descending, and falling. To effectively extract the feature of sEMG signal, we analyzed the WCC between two different sEMG signals to distinguish daily activities. The sEMG signals of RF, ST, TA, and GA muscles were simultaneously recorded from right lower limb of three subjects instructed to execute six experimental activities. Experiment results show significant muscle coherence appearing at the 32th scale. Statistical T test shows that the WCC of RF–ST and ST–TA is statistically different from that of the four other muscle combinations. According to separability and difference analysis, the WCC of RF–ST and ST–TA was selected as the feature. The WCC with SVM exhibits great performance for all activities especially for standing and falling, which feature 100% sensitivity, specificity, and accuracy.

Table 3 Average sensitivity, specificity, accuracy and ROC-AUC for seven features with three classifiers (SEN %, SPE %, ACC %, ROC-AUC)

	SVM				FMMNN				MLP			
Variance	76.92	95.89	86.46	0.85	71.43	74.60	73.12	0.72	77.48	80.26	78.89	0.79
Integral of absolute value	83.33	96.50	89.97	0.90	67.70	97.70	82.78	0.84	76.41	94.35	85.02	0.84
Energy of wavelet packet coefficient	83.33	97.20	90.32	0.91	71.43	95.89	83.69	0.85	78.45	93.47	86.08	0.85
Energy of wavelet coefficient	83.33	97.72	90.58	0.90	76.92	98.59	87.81	0.88	80.14	95.19	87.69	0.88
Auto-regressive coefficient	90.65	93.20	92.01	0.92	87.38	89.73	88.58	0.89	91.14	90.34	90.76	0.91
Recurrent neural networks	91.26	93.43	92.36	0.91	90.74	90.29	90.60	0.91	93.19	92.18	92.73	0.92
Wavelet coherence coefficient	95.98	94.20	95.12	0.94	93.18	89.87	90.57	0.91	94.73	93.41	94.09	0.93

Acknowledgements This work was supported by Zhejiang Public Welfare Technology Research (LGF18F010006), and National Natural Science Foundation of China (61671197, 61673350).

References

1. Thomas O, Sunehag P, Dror G, Yun S, Kim S, Robards M, Smola A, Green D, Saunders P (2010) Wearable sensor activity analysis using semi-Markov models with a grammar. Pervasive Mob Comput 6(3):342–350
2. Turaga P, Chellappa R, Subrahmanian VS, Udrea O (2008) Machine recognition of human activities: a survey. IEEE Trans Circuits Syst Video Technol 18(11):1473–1488
3. Dragan MA, Mocanu I (2013) Human activity recognition in smart environments. In: 2013 19th international conference on control systems and computer science (CSCS), IEEE, pp 495–502
4. Hasanuzzaman FM, Yang X, Tian Y, Liu Q, Capezuti E (2013) Monitoring activity of taking medicine by incorporating RFID and video analysis. Netw Model Anal Health Inform Bioinform 2(2):61–70
5. Mo L, Li F, Zhu Y, Huang A (2016). Human physical activity recognition based on computer vision with deep learning model. In: 2016 IEEE international instrumentation and measurement technology conference proceedings (I2MTC), IEEE, pp 1–6
6. Fleury A, Noury N, Vacher M (2009) Supervised classification of activities of daily living in health smart homes using SVM. In: 2009. EMBC 2009. annual international conference of the IEEE engineering in medicine and biology society, IEEE, pp 6099–6102
7. Zhu C, Sheng W (2011) Wearable sensor-based hand gesture and daily activity recognition for robot-assisted living. IEEE Trans Syst Man Cybern Part A: Syst Hum 41(3):569–573
8. Mukhopadhyay SC (2015) Wearable sensors for human activity monitoring: a review. IEEE Sens J 15(3):1321–1330
9. Bourke AK, Lyons GM (2008) A threshold-based fall-detection algorithm using a bi-axial gyroscope sensor. Med Eng Phys 30(1):84–90
10. Dobkin BH, Dorsch A (2011) The promise of mHealth: daily activity monitoring and outcome assessments by wearable sensors. Neurorehabilit Neural Repair 25(9):788–798
11. Lowe SA, ÓLaighin G (2014) Monitoring human health behaviour in one's living environment: a technological review. Med Eng Phys 36(2):147–168
12. Triloka J, Senanayake SA, Lai D (2017) Neural computing for walking gait pattern identification based on multi-sensor data fusion of lower limb muscles. Neural Comput Appl 28(1):65–77
13. Young AJ, Kuiken TA, Hargrove LJ (2014) Analysis of using EMG and mechanical sensors to enhance intent recognition in powered lower limb prostheses. J Neural Eng 11(5):056021
14. Cheng J, Chen X, Shen M (2013) A framework for daily activity monitoring and fall detection based on surface electromyography and accelerometer signals. IEEE J Biomed Health Inform 17(1):38–45
15. Siantikos G, Giannakopoulos T, Konstantopoulos S (2016) Monitoring activities of daily living using audio analysis and a RaspberryPI: a use case on bathroom activity monitoring. In: International conference on information and communication technologies for ageing well and e-health, Springer, Cham, pp 20–32
16. Ishii A, Kondo T, Yano S (2016) Improvement of EMG pattern recognition by eliminating posture-dependent components. In: International conference on intelligent autonomous systems, Springer, Cham, pp 19–30
17. Kakoty NM, Saikia A, Hazarika SM (2015) Exploring a family of wavelet transforms for EMG-based grasp recognition. SIViP 9(3):553–559
18. Kalnins LM, Simons FJ, Kirby JF, Wang DV, Olhede SC (2015) On the robustness of estimates of mechanical anisotropy in the continental lithosphere: a North American case study and global reanalysis. Earth Planet Sci Lett 419:43–51
19. Lou X, Xiao S, Qi Y, Hu X, Wang Y, Zheng X (2013) Corticomuscular coherence analysis on hand movement distinction for active rehabilitation. Comput Math Methods Med 2013:908591
20. Kopal J, Vyšata O, Burian J, Schätz M, Procházka A, Vališ M (2014) Complex continuous wavelet coherence for EEG microstates detection in insight and calm meditation. Conscious Cogn 30:13–23
21. Imoto R, Migita M, Toda M, Sakurazawa S, Akita J, Kondo K, Nakamura Y (2016) Preliminaly study on coordinated movement mechanism of multiple muscle using wavelet coherence analysis. In: 2016 5th IIAI international congress on advanced applied informatics (IIAI-AAI), IEEE, pp 605–608

22. Mima T, Toma K, Koshy B, Hallett M (2001) Coherence between cortical and muscular activities after subcortical stroke. Stroke 32(11):2597–2601
23. Kakoty NM, Saikia A, Hazarika SM (2015) Exploring a family of wavelet transforms for EMG-based grasp recognition. SIViP 9(3):553–559
24. Guo L, Wu Y, Zhao L, Cao T, Yan W, Shen X (2011) Classification of mental task from EEG signals using immune feature weighted support vector machines. IEEE Trans Magn 47(5):866–869
25. Chen X, Wang ZJ (2013) Pattern recognition of number gestures based on a wireless surface EMG system. Biomed Signal Process Control 8(2):184–192
26. Xi X, Tang M, Miran SM, Luo Z (2017) Evaluation of feature extraction and recognition for activity monitoring and fall detection based on wearable sEMG sensors. Sensors 17(6):1229
27. Roy SH, Cheng MS, Chang SS, Moore J, De Luca G, Nawab SH, De Luca CJ (2009) A combined sEMG and accelerometer system for monitoring functional activity in stroke. IEEE Trans Neural Syst Rehabil Eng 17(6):585–594
28. Sapsanis C, Georgoulas G, Tzes A (2013) EMG based classification of basic hand movements based on time-frequency features. In: 2013 21st mediterranean conference on control & automation (MED), IEEE, pp 716–722
29. Torrence C, Compo GP (1998) A practical guide to wavelet analysis. Bull Am Meteor Soc 79(1):61–78
30. Torrence C, Webster PJ (1999) Interdecadal changes in the ENSO–monsoon system. J Clim 12(8):2679–2690
31. Aloui C, Hkiri B (2014) Co-movements of GCC emerging stock markets: new evidence from wavelet coherence analysis. Econ Model 36:421–431
32. Zhang Y, Liu B, Ji X, Huang D (2017) Classification of EEG signals based on autoregressive model and wavelet packet decomposition. Neural Process Lett 45(2):365–378
33. Han JS, Bien ZZ, Kim DJ, Lee HE, Kim JS (2003) Human–machine interface for wheelchair control with EMG and its evaluation. In: 2003. Proceedings of the 25th annual international conference of the IEEE engineering in medicine and biology society, vol 2, IEEE, pp 1602–1605
34. Karlik B, Olgac AV (2011) Performance analysis of various activation functions in generalized MLP architectures of neural networks. Int J Artif Intell Expert Syst 1(4):111–122
35. Noury N, Fleury A, Rumeau P, Bourke AK, Laighin GO, Rialle V, Lundy JE (2007) Fall detection-principles and methods. In 2007. EMBS 2007. 29th annual international conference of the IEEE engineering in medicine and biology society, IEEE, pp 1663–1666
36. Henderson AR (1993) Assessing test accuracy and its clinical consequences: a primer for receiver operating characteristic curve analysis. Ann Clin Biochem 30(6):521–539
37. Clarke ND, Granek JA (2003) Rank order metrics for quantifying the association of sequence features with gene regulation. Bioinformatics 19(2):212–218
38. Suica Z, Romkes J, Tal A, Maguire C (2016) Walking with a four wheeled walker (rollator) significantly reduces EMG lower-limb muscle activity in healthy subjects. J Bodyw Mov Ther 20(1):65–73
39. Jamwal Y, Singh K (2016) Classification of foot movements using fuzzy logic techniques. In: 2016 7th India international conference on power electronics (IICPE), IEEE, pp 1–5